Characterization of Spatter in Low-Current GMAW of Titanium Alloy Plate

The single stable cathode spot on the base metal, unique to GMA-welded titanium, causes spattering

BY S. T. EICKHOFF AND T. W. EAGAR

ABSTRACT. Severe spattering occurs in low-current GMAW of titanium and titanium alloys. For example, 1.6-mm (1/16-in.) diameter Ti-6Al-4V welding wire spatters at direct current electrode-positive (DCEP) welding currents of less than 240 A, ejecting almost 20% of the filler metal from the weld. Using a high-speed camera, an analysis of metal-droplet transfer in the welding arc was carried out to determine the cause of the spatter.

Spattering is not a result of the plasma jet repelling molten filler metal droplets from the base metal. Spattering follows a regular pattern. The transferring droplets touch down on the base plate and wet the weld pool. At low current levels, a portion of molten welding wire is pinched off and ejected from the vicinity of the weld pool before the droplet incorporates completely, thus causing spatter. As the droplet wets the weld pool, the cathode spot relocates from the weld pool to the top of the transferred, but unincorporated, droplet. Cathode spot relocation from the weld pool to the droplet takes place in approximately 1.1 ms, so the droplet top remains distinguishable from the weld pool for at least this length of time. The current levels that are associated with spatter are associated with globular transfer of filler metal droplets, and comparatively slow droplet wire-to-plate transfer velocities. Below 240 A, droplet transfer velocities are typically 130 cm/s (4.3 ft/s). The low droplet transfer velocities associated with low-current welding allow a sufficiently lengthy incorporation lifetime for the spatter mechanism to operate.

The force required to eject a spatter droplet with an acceleration of between 430×10^3 cm/s^2 and 930×10^3 cm/s^2 is between 240 and 520 dynes. Forces due to aerodynamic drag of the streaming plasma and the reaction force of the strong cathode jet can account for no more than 10 dynes apiece. Forces due to electromagnetic pumping can account for several hundred dynes of ejection force, provided the welding current is entirely shunted through the unincorporated droplet.

The ability of the filler metal droplet to briefly shunt the welding current depends on the nature of the cathode spot. The thermionic electron emission mechanism found in titanium produces a single, stable cathode spot on the base metal, which is unique among the metals commonly GMA welded. This emission mechanism accounts for the low-current spatter occurring in GMA-welded titanium alloys.

S. T. EICKHOFF is with Wyman-Gordon Co., Worcester, Mass. T. W. EAGAR is a Professor in the Department of Materials Science and Engineering, MIT, Cambridge, Mass.

Paper presented at the 70th Annual AWS Meeting, held April 2–7, 1989, in Washington, D.C.

KEY WORDS

GMAW Spattering
Low-Current GMAW
Titanium GMAW Spatter
Cinematic Analysis
High-Speed Movies
Droplet Transfer
Transfer Velocities
Cathode Spot Relocation
Electromagnet Pumping
Droplet Ejection Force

Introduction

In the mid-sixties, research into gas metal arc welding (GMAW) of heavy titanium plate was spurred by interest in building naval hulls from such material. The welding parameters were selected for rapid filler metal deposition in a flat position. Using 1.6-mm (0.062-in.) diameter electrodes, welding currents in excess of 300 A, direct current, electrode-positive (DCEP) were typically selected, using a shielding gas of pure argon. These high welding currents gave smooth spray transfer across the welding arc. Use of lower currents, giving globular transfer, produced an unstable arc and spattering (Refs. 1–4).

The use of high welding currents is acceptable in flat position mechanized welding, but lower welding currents, which give smaller weld pools or allow slower travel speeds, are desirable in manual GMAW or out-of-position welding. Previous attempts to decrease the welding current without producing the heavy spatter associated with globular transfer in titanium have concentrated on pulsed-current GMAW (Refs. 5, 6). Pulsed-current GMAW typically uses a welding-current modulation frequency ranging from 50–1000 Hz to achieve spray transfer behavior at low mean-current levels. These efforts have been partially successful but have been hampered by a lack of understanding as to the nature of the spatter that occurs in titanium welding.

At least one previous researcher has noted the presence of an intense plasma jet, which originates at the titanium base metal in DCEP GMAW (Ref. 6). Figure 1 presents a photo of the plasma jet as found on titanium. The presence of this cathode jet has led to the suggestion that the plasma jet repels molten filler metal droplets from the weld pool. This study will demonstrate that the repulsion of filler metal droplets is not a result of momentum transfer from the gas jet to metal droplet, but it is a result of Lorentz-type pinch forces acting upon filler metal droplets when they touch down at the weld pool.

Experimental Design

A series of 11 bead-on-plate welds was made on 1.3-cm (0.5-in.) thick titanium alloy (Ti-6Al-4V) plate. Pure argon shielded the arc and a 1.6-mm (0.062-in.) diameter Ti-6Al-4V electrode was used. No more than 1 h prior to welding, the titanium plate was surface ground to remove ox-

Fig. 1 — The intense cathode plasma jet that has formed on a titanium baseplate during GMAW. The jet can be seen originating on the weld pool. The welding electrode is seen at the top of the photo. The bright backlighting is due to the laser beam. 1.6-mm Ti-6Al-4V electrode. 235 A.

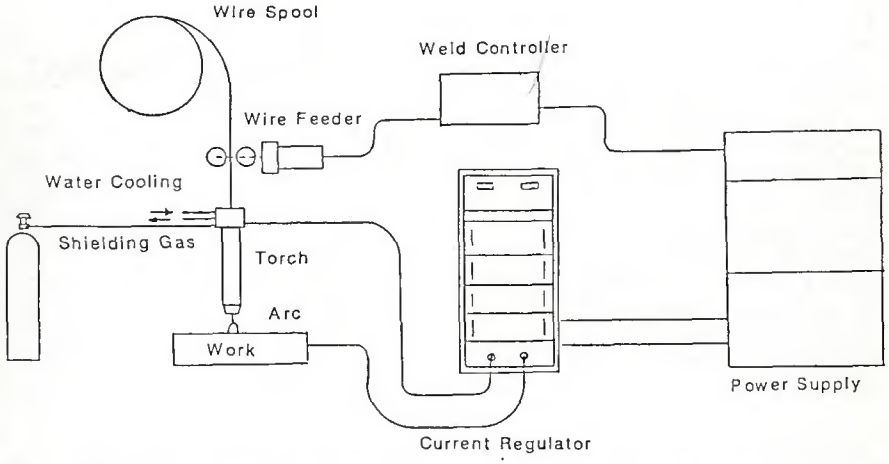

Fig. 2 — The welding apparatus was instrumented to facilitate data collection, but was mainly commercial equipment. The transistorized welding power regulator was constructed for this project.

ides and washed with reagent grade methanol to remove grinding debris.

Observation of the welds was facilitated by a laser backlighting system developed in the MIT Materials Joining Laboratory (Ref. 7). A high-speed camera capable of filming 6000 frames per second was positioned to record the transfer of molten metal from the end of the welding wire to the weld pool. A series of lenses and filters allowed the selective removal of arc light and passage of laser light to the film. Some arc light was allowed to pass the filters to show the location of the plasma jets, which are the most luminous portion of the arc plasma, without obscuring the images of the transferring droplets.

Time information was recorded using pulsed LEDs on the margin of the films. The LEDs were strobed on for 0.167 ms then off for 0.833 ms so that a series of streaks appears at the edge of the film at 1-ms intervals. This allows droplet velocity to be measured by comparing droplet position with elapsed time on a frame-by-frame basis. Inaccuracies were introduced by the finite length of time required to expose any given frame of the film. Nonetheless, velocities can typically be measured by this technique to an accuracy of 6%. Acceleration measurements are somewhat worse due to the very short time increments that must be used in acceleration measurements. A variation of nearly 50% is the best that can be expected at a framing rate of 6000 Hz.

In addition to the film record, welding current and arc voltage were recorded on an oscillographic recorder with a 1-kHz bandwidth. This device provided a check on the accuracy of the welding parameters and also allowed comparison with the time information recorded as streaks on the high-speed film. The formation and separation of individual filler droplets at the electrode appears as troughs and peaks on the arc voltage trace.

The welding current was produced by a constant current power supply, feeding a transistorized current regulator with a 600-A rating. The current regulator was built in the MIT Materials Joining Laboratory specifically for welding research (Ref. 8). It is capable of producing any current waveform of bandwidth <3 kHz, and in addition, is instrumented for recording arc current and voltage. A commercial weld controller, voltage feedback-controlled electrode feed motor, and GMA welding gun completed the welding equipment. The base metal sample was clamped to a water-cooled welding platen prior to welding. The platen automatically traversed the sample beneath the welding gun, allowing it to remain stationary. The welding apparatus is shown schematically in Fig. 2.

Observations

The spattering behavior of titanium is strongly dependent on welding current. At constant voltage, spatter ceases above a cut-off welding current, which correlates with the change from globular transfer to spray transfer.

Transfer Frequency

The change in droplet transfer mode can be determined from Fig. 3, showing the dependence of droplet transfer frequency on welding current at constant electrode feed speed. (Ordinarily, GMA welding is done using a constant potential power supply, and current is controlled by

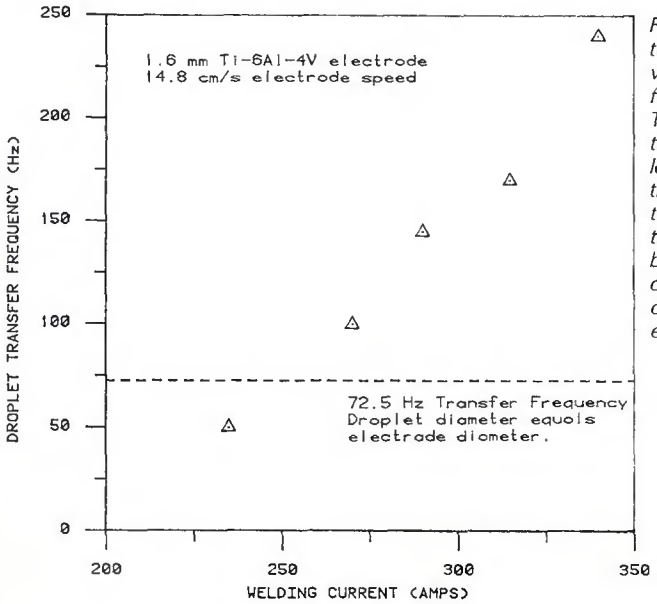

Fig. 3 — Droplet transfer frequency vs. welding current for constant voltage. This graph shows the welding current level when globular transfer gives way to projected transfer, as judged by the relative diameters of the droplet and the electrode.

wire feed rate.) The horizontal line shows the calculated cut-off transfer frequency below which the transferring droplet must be larger than the electrode diameter of 1.6 mm. This line was calculated assuming conservation of mass at the fixed wire feed speed of 14.8 cm/s (350 in./min). Globular transfer is characterized by filler metal droplets somewhat larger than the electrode diameter. At the cut-off frequency, transition from globular to spray transfer occurs. In the case of 1.6-mm-diameter titanium alloy electrodes, the transition welding current is between 240 and 250 A.

Transfer Velocity

As the transfer mode changes from the gravity-dominated globular transfer to the pinch-force-dominated spray transfer, the velocity of the droplet as it transfers across the arc length is seen to increase. Figure 4 shows the range of velocities observed in droplets transferring across the arc in welds made between 200 and 350 A at 38 V using 1.6-mm-diameter electrodes. The cut-off transfer velocity above which no spatter occurs is 130 cm/s (51 in./s).

Figure 4 records average data from 2–3 droplets from each weld, since there is a spread of velocities within each weld. Welds made at currents above 245 A have essentially no droplets transferring at less than 130 cm/s. Furthermore, welds made at lower currents have large proportions of droplets transferring at low velocities, and a correspondingly large number of spatter droplets ejected from the weld pool.

Inertial Time Constant

Transfer velocity and droplet diameter are both strongly dependent on welding current, and the effects of each on spatter formation are difficult to separate from the effects of the other. A better measure of spatter forming strength than either transfer velocity or droplet diameter considered separately is the inertial time constant t_i. This constant is a measure of the time for a droplet to interact with the weld pool, defined as droplet diameter divided by droplet transfer velocity. Physically, t_i is a measure of the time for a droplet to transverse its own diameter. Figure 5 shows the cut-off time constant.

Spatter Sequence

The formation of a filler metal droplet on the electrode is the first event in a sequence that ultimately leads to spattering. In low-current spatter, the droplet will grow to a diameter larger than the electrode before it is separated and approaches the plate. As noted previously, the velocity that the transferring droplet attains is dependent on the welding current – Fig. 4.

When the transferring droplet touches down on the weld pool, the cathode plasma jet is seen to reposition itself within 0.002 s to the top of the droplet from whatever location it held previously. Since the cathode jet originates at a localized point on the weld pool that is the cathode spot, the new origin of the cathode jet indicates a new current path. Simultaneously, the droplet begins to incorporate into the weld pool. Within approximately 10 ms, a portion of the droplet separates from the surface of the weld pool and accelerates away from the base metal as spatter.

Spattering follows a regular pattern, with one spatter droplet forming from each transferring droplet. A typical spatter droplet is measured to be 0.62 mm (0.024 in.) in diameter and is seen to accelerate away from the weld pool at between 430×10^3 and 930×10^3 cm/s^2, reaching a velocity of 260 cm/s (8.5 ft/s) in a time between 0.28 ms and 0.60 ms. Taking the density of molten titanium alloy to be 4.5 g/cm^3, the force ejecting the spatter droplet is between 240 and 520 dynes.[1] The spattering process is shown in Fig. 6.

The ejected spatter droplets typically follow the direction of the cathode jet. The incoming droplets, contrary to intuition, are not deflected by the cathode jet. The transferring droplets do not, in general, encounter the cathode jet at all until they touch down on the base metal – Fig. 1. The ejected spatter droplets, however, originate at the same site as the cathode jet, and so are influenced by the jet throughout their flight.

Calculations and Analyses

Force Estimation

The magnitude of the forces ejecting the spatter droplet can be estimated. Three ejecting forces will be considered. Electromagnetic pumping due to the constriction of a fluid conductor by the self-magnetic field of the current will be des-

1. Dyne is the cgs unit of force, equal to 10^{-5} newton, or about 36 millionths of an ounce.

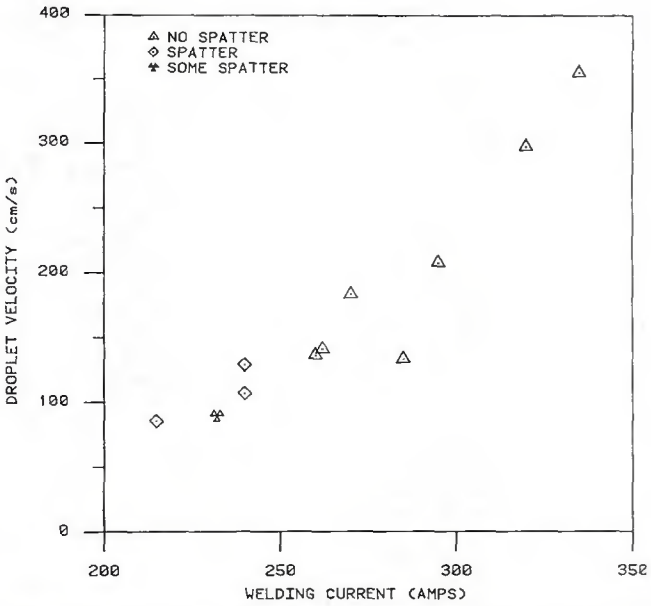

Fig. 4 – Droplet transfer velocity vs. welding current. This graph shows the increase in droplet transfer velocity with increasing welding current. Projected transfer gives much higher velocities than globular transfer.

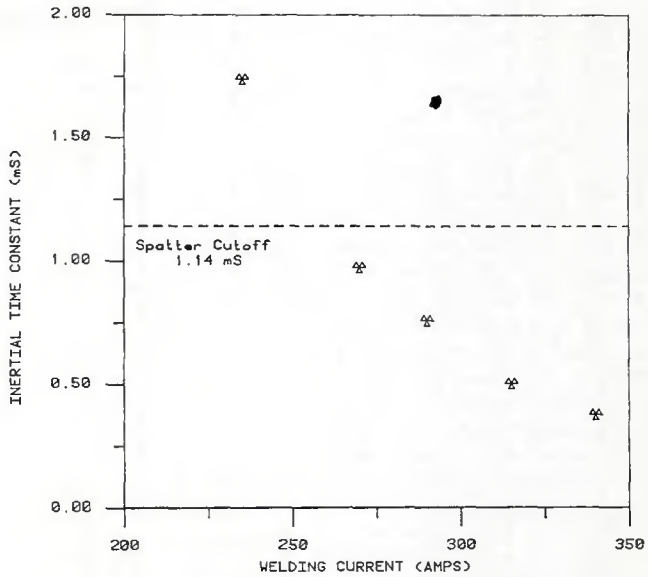

Fig. 5 – Inertial time constant vs. welding current. This graph shows the decreasing interaction time for the transferring droplet to be in contact with the weld pool but not yet incorporated.

ignated F_L, for Lorentz force. Lorentz forces play an important role in separating filler metal droplets from the electrode, but they are also important in spatter formation in titanium. The hydrodynamic drag force of the plasma stream flowing past the molten droplet will be noted as F_s, for the streaming force. The final force to be considered, F_j, is the reaction force of the plasma jet impinging on the droplet; a force resulting from momentum transfer from jet to droplet. Figure 7 summarizes these forces.

The forces affecting the ejected droplet can be divided into two groups. The first group operates before the droplet leaves the base metal, and is responsible for separating the droplet from the weld pool. The forces F_s and F_L can be considered to be in the first group. The second group of forces operates after the spatter droplet leaves the weld pool; F_j is in the second group.

F_S Force

If we consider the droplet to be an approximately spherical body in a stream of plasma, we can estimate F_s. The spherical approximation is reasonable; as the droplet is pinched off, it resembles a sphere with a neck attaching it to the weld pool. At any time before pinch off, however, the following analysis will overestimate F_s, since not all of the droplet is exposed to the plasma stream.

The coefficient of drag, C_D, for a sphere of diameter D, in a stream of velocity U and density ρ, is known as a function of the Reynolds number, N_{Re}, which can be determined as,

$$N_{Re} = \frac{\rho U D}{\mu}$$

In the case of an argon plasma at approximately 10,000 K, fluid density is 4×10^{-5} g/cm^3, and viscosity is 2.9 m poise (Ref. 9). Assuming a 100 m/s (328 ft/s) plasma velocity, and using the 0.62-mm (0.024-in.) droplet diameter, $N_{Re} = 8.55$, and therefore $C_D = 5.0$, one can calculate F_s from,

$$C_D = \frac{F_s}{(1/2\rho\, U^2)\ A}$$

where A = frontal area of the drop. Solving this equation, F_s is found to be less than 30 dynes.

F_L Force

Amson (Ref. 10) has analyzed the Lorentz forces on a droplet being pinched off of a wire, but the analysis applies equally well to the situation of a droplet being pinched off of a weld pool. Amson quantifies the Lorentz force due to a welding current I as

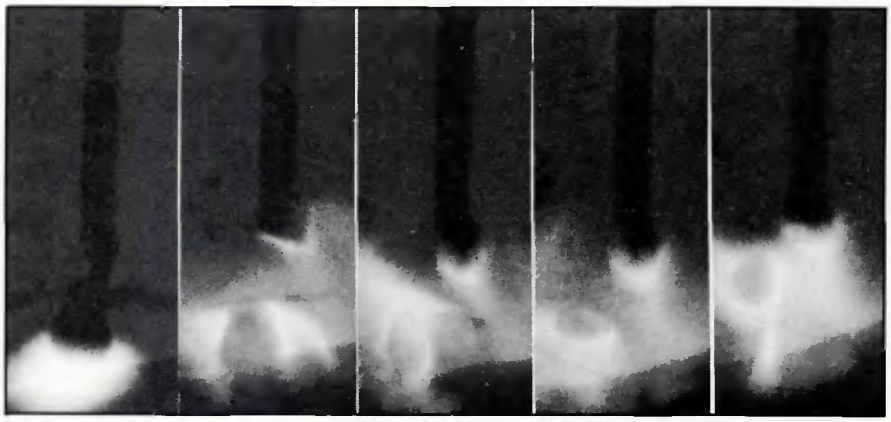

Fig. 6 — Rejected transfer of a titanium droplet, showing the droplet touching down, the cathode jet forming on top of the droplet, and finally, a portion of the droplet being pinched off of the weld pool and ejected. Parameters are: 1.6-mm-diameter electrode, 205-A current at 25 V. Time between frames is approximately 0.010 s. Droplet transfer velocity is 120 cm/s.

$$F_L = \frac{\mu_0}{(4\pi)} I^2 n(\beta)$$

where μ_0 = the permeability constant of free space, 12.6×10^{-7} H/m, and $n(\beta)$ = a geometric constant. The factor β is an angular timing parameter for droplet detachment. When $\beta = 0$ deg, the droplet is as yet unformed. At $\beta = 150$ deg, the droplet is suspended only by a filament.

For an exact analysis of $n(\beta)$, the shape of the droplet in question must be known, as must be the extent of the current conducting area on the top of the droplet. Although shape information is readily available, information on the conducting area can only be estimated.

Amson has calculated $n(\beta)$ for a droplet pinched off of a wire — Fig. 8. It is assumed that Amson's values for $n(\beta)$ are not very different from the actual values for the present case. The $n(\beta)$ value ranges from 0.18 to large values ($n(\beta) >> 1$) as the droplet necks down prior to separation from the wire. As the separation proceeds, the Lorentz force increases dramatically until the break occurs. For the droplet under consideration in this paper, the welding current is 230 A, therefore

$$F_L = 529[n(\beta)] \text{ dynes}$$

Thus, depending on $n(\beta)$, F_L ranges from 100 to 1000 dynes during the process of spatter formation. Clearly, it is reasonable to estimate F_L to be on the order of several hundreds of dynes by the time the spatter droplet separates from the weld pool.

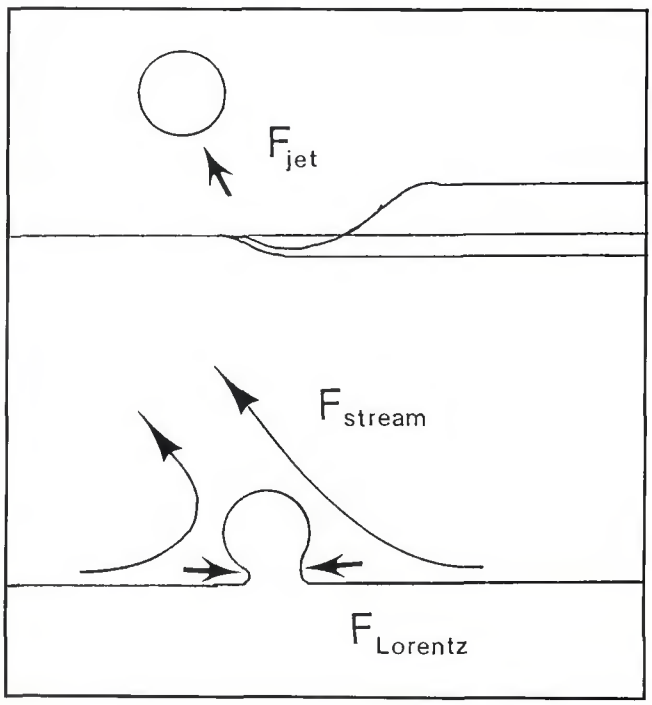

Fig. 7 — The forces acting on an unincorporated droplet to accelerate it away from the baseplate.

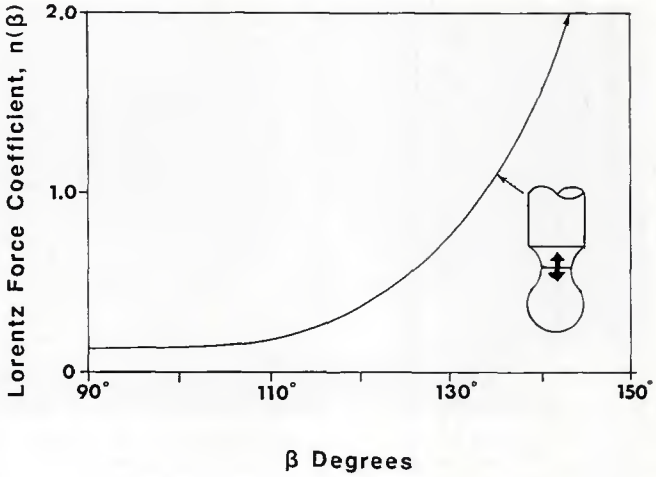

Fig. 8 — The dependence of n(β) on the separation angle. After Amson, the separation angle indicates the completeness of spherical droplet formation. 0 deg is a square-ended electrode with no droplet. 180 deg is a free spherical droplet.

Fig. 9 — Impingement of the cathode plasma jet on a transferring droplet. Welding current is 260 A at 34 V. Electrode is 1.6-mm diameter.

F_j Force

The second group of spatter ejection forces occurs when the droplet is separated from the plate and is moving away from the weld pool. In this regime, the spatter droplet is no longer a part of the conducting circuit, therefore $F_L = 0$. Furthermore, the cathode jet that develops at the weld pool impinges on the droplet as it is in flight. The droplet cannot be assumed to be simply entrained in the plasma stream, affected only by hydrodynamic drag forces. Instead, the highly concentrated plasma jet transfers momentum directly to the drop. The film record shows that the plasma jet diameter is smaller than the spatter droplet diameter, and that the plasma jet is redirected when it hits the droplet — Fig. 9. Little of the jet plasma goes past the droplet to create a drag force. In short, F_s is negligible in this regime, but F_j, the impingement force, is not.

If a restricted jet of cylindrical cross-section impinges on a droplet much larger than itself, then a simple fluid-mechanical estimation of force can be made. Figure 10 shows the geometry of this problem. In the x-direction, the momentum flux of the incoming jet is

$$F_j = \rho\, AU^2 \left(\frac{\text{g-cm}}{\text{sec}^2}\right)$$

where A is the impacting area of the jet.

The diameter of the plasma jet can be estimated from the film records of welds to be 0.5 mm (−0.1/+0.2) (0.02 in.). Assuming a 100 m/s (328 ft/s) jet velocity, this gives $F_j = 8$ dynes. Assuming a larger and faster jet of 0.75 mm (0.03 in.) diameter and 200 m/s (656 ft/s) velocity raises F_j to 70 dynes. Due to the extreme sensitivity of the force calculation to the estimated values of jet diameter and velocity, the best estimation of F_j is that it is of the order of tens of dynes, which is comparable to F_s in the first regime.

Analysis of Emission Mechanism

The force calculations above demonstrate that the only mechanism of sufficient strength to eject spatter droplets with the observed acceleration is the electromagnetic pumping associated with the welding current. The F_L force calculation shows that several hundred dynes of force can be applied to the spatter droplet from electromagnetic pumping. The F_L force is at least an order of magnitude greater than other forces affecting the droplet, and is approximately equal to the forces observed to eject the droplet.

The F_L force calculation assumes that after droplet touchdown, the cathode spot transfers to the top of the transferred, but unincorporated, droplet. The entire welding current must then flow through the droplet. This behavior is possible only if cathode behavior is such that electron emission can occur 1) at a site no larger than the droplet top, which is less than 2 mm (0.08 in.) in diameter, and 2) at a site that is stable on top of the droplet before droplet ejection, for a period of approximately 5 ms.

Two broad categories of electron emission behavior are commonly identified in metals, cold-cathode emission and thermionic emission (Ref. 11). These mechanisms are not mutually exclusive. Electron emission may take place via both mechanisms simultaneously, although it is often possible to determine a dominant mechanism.

In thermionic emission, the energy used to remove electrons from the bulk metal and place them in free space comes from the thermal energy of the electrons. Electrons can be "boiled out" of a metal with a current density, J, which is related to metal temperature, T, by the Richardson-Dushman equation,

$$J(T) = AT^2 \exp\left(-\frac{\Phi e}{kT}\right)\left(\frac{\text{amps}}{\text{cm}^2}\right)$$

where A is a constant, k is Boltzman's constant and Φ is the work function of the metal (Ref. 12).

Cold-cathode emission relies on an external energy source to remove electrons from the bulk metal. Photoemission is an

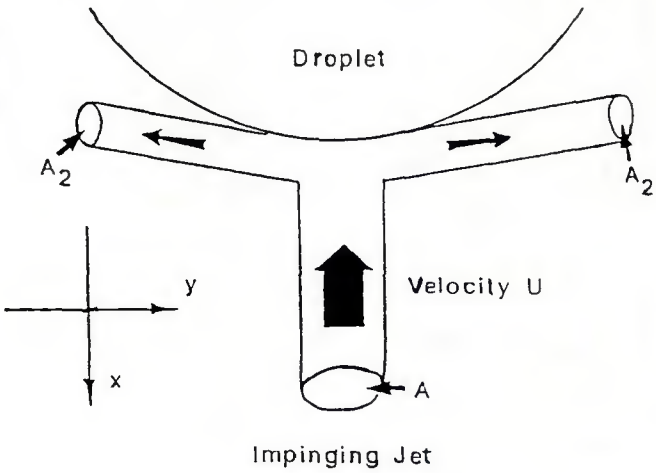

Fig. 10 — Geometry of plasma jet impingement on a transferring droplet.

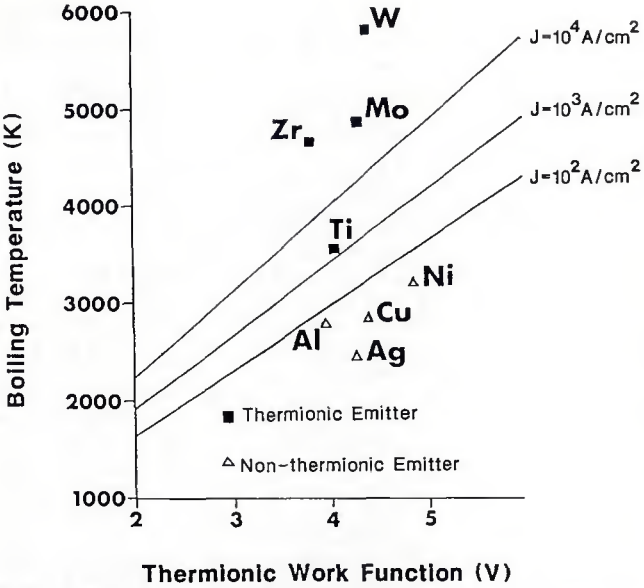

Fig. 11 — Guile's graph showing the ability of various metals to behave as efficient thermionic emitters. Metals above the 10^7 A/m² line may act as thermionic emitters in the welding arc.

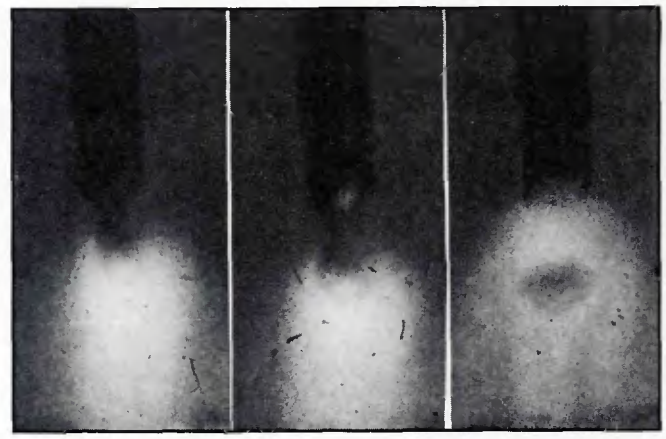

Fig. 12 — An intense cathode plasma jet does not form when welding aluminum. Numerous mobile cathode spots characteristic of a cold-cathode emitter result in a very diffuse arc with no cathode jet.

example of a cold-cathode process that uses the energy of incident photons, but the most important cold-cathode process in an electric arc is field emission. In field emission, an external electric field strips electrons out of the bulk metal with a current density, J, which can be related by the Fowler-Nordheim equation to the electric field strength, E, at the metal surface,

$$J(T) = \frac{E}{e\Phi}\exp\left(-\frac{Be\Phi}{E}\right)\left(\frac{\text{amps}}{\text{cm}^2}\right)$$

where B is a constant, e is the electronic charge, and Φ is the work function of the metal (Ref. 13).

Emitted current densities of 10^6–10^7 A/cm² have been reported in field emitters, while somewhat smaller current densities are observed in thermionic emitters, 10^4–10^5 A/cm² (Ref. 14). Given a welding current of 250 A, a field emitter would need to sustain an emitting area of 2.5×10^{-4} cm², equivalent to a circular patch with a 0.2-mm (0.008-in.) diameter. A thermionic emitter would need a circular patch of approximately 1-mm (0.04-in.) diameter to maintain a similar current level. Thus, either thermionic or field emission could produce a spot small enough to reside on the unincorporated filler droplets.

Emitting site lifetimes are related to energy reduction criteria. An electric arc will minimize the energy required for it to exist by 1) minimizing the current path length, and 2) anchoring at the most efficient electron emission sites on the cathode.

Thermionic emitting site efficiency is dependent on temperature. All other factors being equal, the hottest site on the cathode will emit the greatest current by this mechanism. Current flowing at a hot site will maintain or raise the temperature of the emitting site by resistive heating. A thermionic emitting site, once established, is very stable because current flow reinforces the conditions for efficient thermionic emission.

The work function, through the Richardson-Dushman equation, strongly influences the electron evaporation rate, which in turn sets the operating temperatures of the emission site. If emission is possible at a lower temperature than that which is attained elsewhere in a conductor due to joule heating, then the emission site will act as a heat sink. For a solid electrode, Savage, *et al.* (Ref. 15), demonstrated that the current emitting site of a thoriated tungsten welding electrode acts as a heat sink, in the same manner as a water-cooled collet holding the other end. Savage observed that at high currents, the thoriated electrode melts at a point between the two ends, not at the emission site adjacent to the arc. Savage also noted that a pure tungsten electrode, by contrast, melts first at the emitting site. At the steady state, heat input from joule heating, radiation from the arc, and conduction from the arc is balanced by heat output due to electron evaporation, radiation to the general surroundings, and conduction through the electrode toward the collet. The complementary flow of heat generated by joule heating in the conductor vs. heat required to operate the thermionic emission site determines what part of the electrode melts first.

In a planar liquid cathode, convective heat transfer prevents joule heating "hot spots," so that one would expect the emitting site to be the hottest point on the cathode surface. The Peclet number, N_{Pe}, which is the ratio of convective heat flow to conductive heat flow, is

$$N_{Pe} = \frac{Lu\rho C_p}{k}$$

where L is a characteristic dimension, u = velocity, p = density, C_p = specific heat, and k = thermal conductivity. In a solid, $N_{Pe} = 0$, since the velocity equals zero. For molten titanium in a weld pool, with a pool diameter of about 1 cm (0.4 in.), flow rates of 10 cm/s (Ref. 16), k = 0.2 J/cm-K, ρ = 4.11 g/cm³, and C_p = 0.7 J/g-K (Ref. 17), the Peclet number is calculated to be of the order of 10^2. The observed stability of the cathode spot on a titanium weld pool demonstrates that despite cooling by electron evaporation, the emission site remains the hottest point on the weld pool.

A field emitting site is favored at locations of high field strength or low work function. The Fowler-Nordheim equation predicts field strengths on the order of 10^6 V/cm to account for the observed high current density, and yet in the arc, field strengths of no more than 10^4 V/cm are observed macroscopically (Ref. 13). Suggested mechanisms to account for field intensification at the cathode surface rely on the existence of a rough insulating impurity layer on the metal surface, in particular, a layer of the self-oxide of the cathode material. The stabilizing influence of small amounts of oxygen on arcs struck on steel and on aluminum supports the role of an oxide in field emission processes. The action of an electric arc at the cathode rapidly disperses the oxides and other impurities, decreasing the emission efficiency of the site, and eventually destroying the site. Field emitting cathodes are characterized by short individual site lifetimes of <1 ms, and rapid movement of the arc, as old emitting sites are de-

stroyed and new sites form.

The nature of electron emission on a given metal is dependent on the temperature of the metal, and the presence of impurities, particularly oxides, at the metal surface. Figure 11 shows the relation of the melting point of several metals with the thermionic work function, as plotted by Guile (Ref. 13). The line shows the lower limit of thermionic emission. Below the line, metals melt before significant thermionic emission occurs. Metals above the line are sufficiently refractory to sustain significant thermionic emission.

Aluminum is an example of a nonthermionic metal—Fig. 12. Field emission is expected and is observed on aluminum during welding. Titanium melts at a sufficiently high temperature to be a thermionic emitter, and the extremely stable cathode spot of titanium, which gives rise to a well-developed plasma jet, is proof of thermionic behavior.

According to Fig. 11, titanium is the only commonly welded metal that will support thermionic emission. Other less commonly welded metals, such as hafnium and zirconium, also exhibit the strong cathode jet and spattering as found in titanium (Ref. 18).

Conclusions

The stability of the thermionic emission site at the top of the unincorporated weld droplet is responsible for the spattering observed in low-current GMAW of titanium plate. The thermionic electron emission found in titanium alloys allows the entire welding current to be shunted through the filler metal droplet as it touches down on the weld pool. Lorentz-type pinch forces then expel a large portion of the droplet from the weld pool.

Future attempts to eliminate spatter in titanium must focus on destabilizing the cathode spot. The top of the unincorporated filler metal droplet must not be a stable emitting site.

Acknowledgments

The authors wish to express their appreciation to both the Office of Naval Research (Contract N00014-80-C-0384) and the Department of Energy (Contract DE-FG02-85ER-13331) for support of their research.

References

1. Stark, L. E., Bartolo, L. J., and Porter, H. G. 1962. Welding on one-inch-thick Ti-6Al-4V plate. *Welding Journal* 41(9):805-814.

2. Wolfe, R. J., Nagler, H., Crisci, J. R., and Frank, A. L. 1965. Out-of-chamber welding of Ti-7Al-2Cb-1Ta alloy titanium plate. *Welding Journal* 49(10):443-s to 457-s.

3. Stark, L. E. 1966. Weldability of Ti-7Al-2Cb-1Ta plate. *Welding Journal* 50(2):70-s to 81-s.

4. Mitchell, D. R., and Feige, N. G. 1967. Welding of alpha-beta titanium alloys in one-inch plate. *Welding Journal* 46(5):193-s to 202-s.

5. Salter, G. R., and Scott, M. H. 1967. The pulsed inert gas metal arc welding of 1-in.-thick titanium 721 alloy. *Welding Journal* 46(4):154-s to 167-s.

6. Ries, D. E. 1983. Gas metal arc welding in titanium. M.S. thesis. MIT Department of Materials Science and Engineering.

7. Allemand, C. D., Schoeder, R., Ries, D. E., and Eagar, T. W. 1985. A method of filming metal transfer in welding arcs. *Welding Journal* 65(1):45-47.

8. Galler, D., Kusko, A., and Converti, J. 1981. A fast response transistor current regulator for welding research. IEEE IAS Annual Meeting, Philadelphia, Pa.

9. Devoto, R. 1973. Transport coefficients in ionized argon. Phys. of Fluids 16(5):616-623.

10. Amson, J. C. 1965. Lorentz force in the molten tip of an arc electrode. *Brit. JAP,* 16, pp. 1169-1179.

11. Murphy, E. L., and Good, R. H., Jr. 1956. Thermionic emission, field emission and the transition region. *Phys. Rev.* 102(6):1464-1473.

12. Finkelnburg, W., and Maecker, H. 1962. Electric arcs and thermal plasmas. *ARL 302,* USAF 1971. Arc electrode phenomena. *Proceedings of IEE,* IEE Reviews, 118(9R), p. 1131.

13. Guile, A. E. 1971. Arc electrode phenomena. *Proceedings of IE,* IEE Reviews, 118(9R), p. 1131.

14. Ecker, G. 1961. Electrode components of the arc discharge. *Ergebnisse der Exacten Naturwissenschaften,* F. Hund, ed., Springer-Verlag, Berlin, West Germany.

15. Savage, W. F., Strunk, S. S., and Ishikawa, Y. 1965. The effect of electrode geometry in gas tungsten arc welding. *Welding Journal* 49(11):489-s to 496-s.

16. Tsao, K. C., and Wu, C. S. 1988. Fluid flow and heat transfer in GMA weld pools. *Welding Journal* 67(3):70-s to 75-s.

17. 1983. *Smithell's Metals Reference Book,* 6th ed.; E. Brandes, ed.; Butterworth and Co., Ltd., London, U.K., pp. 13-14.

18. Cooksey, C. J., and Milner, D. R. 1966. Metal transfer in gas shielded metal arc welding. *Symposium on the Physics of the Welding Arc,* IIW, London, U.K. pp. 123-132.

Invitation to Participate in the Inaugural Meeting of the AWS G2 Committee on Joining Metals & Alloys

This committee was approved at the Spring meeting of the AWS Technical Council. The Scope of the committee is as follows:

To survey industry groups and identify need for information on joining specific families of alloys. Identify and select specific groups or classes of alloys that are sufficiently alike so that a single standard can be logically prepared on the joining of these metals.

Recruit additional committee and subcommittee members to prepare the selected standards.

The first meeting of the G2 Committee will be held on November 5 and 6, 1990 in Newport News, Va. Anyone interested in attending the meeting should contact Leonard P. Connor of the American Welding Society (800) 443-9353.